NEUROSCIENCE
RESEARCH ARTICLE
A. Mehmood et al. / Neuroscience 545 (2024) 69–85

Utilizing Siamese 4D-AlzNet and Transfer Learning to Identify Stages of Alzheimer's Disease

Atif Mehmood, [a,b] **Farah Shahid,** [a,b,*] **Rizwan Khan,** [a] **Mostafa M. Ibrahim** [c] **and Zhonglong Zheng** [a,*]

[a] *School of Computer Science and Technology, Zhejiang Normal University, Jinhua 321004, China*

[b] *Zhejiang Institute of Photoelectronics & Zhejiang Institute for Advanced Light Source, Zhejiang Normal University, Jinhua, Zhejiang 321004, China*

[c] *Department of Electrical Engineering, Faculty of Engineering, Minia University, Minia 61519, Egypt*

Abstract—Alzheimer's disease (AD) is the general form of dementia, leading to a progressive neurological disorder characterized by memory loss due to brain cell damage. Artificial Intelligence (AI) assists in the early identification and prediction of AD patients, determining future risks and benefits for radiologists and doctors to save time and cost. Since deep learning (DL) approaches work well with massive datasets and have recently become helpful for AD detection, there remains an area for improvement in automating detection performance. Present approaches somehow addressed the challenges of limited annotated data samples for binary classification. This contrasts with prior state-of-the-art techniques, which were constrained by their incapacity to capture abstract-level information. In this paper, we proposed a Siamese 4D-AlzNet model comprised of four parallel convolutional neural network (CNN) streams (Five CNN layer blocks) and customized transfer learning models (Frozen VGG-19, Frozen VGG-16, and customized AlexNet). Siamese 4D-AlzNet was vertically and horizontally stored, and the spatial features were passed to the final layer for classification. For experiments, T1-weighted MRI images comprised of four distinct subject classes, normal control (NC), mild cognitive impairment (MCI), late mild cognitive impairment (LMCI), and AD, have been employed. Our proposed models achieved outstanding accuracy, with a remarkable 95.05% accuracy distinguishing between normal and AD subjects. The performance across remaining binary class pairs consistently exceeded 90%. We thoroughly compared our model with the latest methods using the same dataset as our reference. Our proposed model improved NC-AD and MCI-AD classification accuracy by 2% 7%.

Key words: siamese-4D-AlzNet, deep learning, classification, late mild cognitive impairment, transfer learning.

INTRODUCTION

Alzheimer's disease (AD) is a devastating neurological illness that is rapidly increasing in prevalence across the world. This disorder is becoming increasingly common as the world population ages, which has severe consequences for individuals, communities, and economies (J. T. Wang et al., 2022). In 2020, it is predicted that there will be over 50 million individuals living with dementia globally, with AD accounting for almost two-thirds of all cases. The number of people living with dementia is expected to rise to 152 million by 2050, putting a heavy burden on healthcare services and infrastructure (Heising and Angelopoulos, 2022). The chance of developing Alzheimer's increases with age. After age 65, the disease incidence doubles around every five years (Wen et al., 2020). Medical costs, long-term care costs, and productivity losses were all factors in the worldwide projection of one trillion US dollars for dementia care in 2019. Caregiving is difficult for AD patients (Mingxia Liu et al., 2019b). Over 11 million unpaid caregivers in the United States assist those with AD and other forms of dementia. Alzheimer's disease remains incurable after decades of study (Hazarika et al., 2023). However, there have been substantial efforts to discover disease-modifying therapeutics. Although significant, the global investment in Alzheimer's research remains insufficient compared to the illness's effect (Puig-Parnau et al., 2023). In AD, amyloid plaques and tau tangles build up in the brain, causing cell loss and cognitive deterioration (Joy et al., 2018).

*Correspondence to: F. Shahid and Z. Zhonglong, School of Computer Science and Technology, Zhejiang Normal University, Jinhua 321004, China.
E-mail addresses: farahatif@zjnu.edu.cn (F. Shahid), zhonglong@zjnu.edu.cn (Z. Zheng).

Abbreviations: AD, Alzheimer's disease; AI, artificial intelligence; DL, deep learning; LMCI, late mild cognitive impairment; MCI, mild cognitive impairment; NC, normal control.

https://doi.org/10.1016/j.neuroscience.2024.03.007
0306-4522/

Medical imaging modalities encompass a range of techniques, such as MRI, PET, fMRI, and EEG images. The utilization of MRI-scanned data offers significant advantages due to their enhanced spatial resolutions, enabling the visualization of image features that help diagnose various diseases (Ferreira et al., 2018). At the macroscopic level, alterations in brain morphology are of significant importance in identifying and assessing AD, often characterized by the presence of front temporal lobe atrophy (Hampstead et al., 2022). Reduced brain tissue within this specific region leads to a decline in the functioning of the amygdala and hippocampus (Xiao et al., 2023). Experts are investigating strategies to identify this condition earlier to improve therapeutic interventions (Plachez et al., 2023). Recent research suggests that the disease may start damaging the brain years before symptoms become apparent, emphasizing the importance of early detection and intervention (Peng et al., 2022).

Medical experts face many challenges during manual processing, and many other physical checks cannot produce sufficient results. Because monitoring the molecular changes in the different regions of the brain is very difficult to access. Moreover, manual procedures require a longer time and also need direct interaction between patients (Grundman et al., 2002). When neurological images are processed correctly, suitable features and diagnostics that can be effectively used to differentiate different stages of AD may be obtained. According to the brain's complex structure, getting the correct information from the other brain regions is very challenging for multiple traditional neuroimaging tools and preprocessing pipelines (Manhua Liu et al., 2018). Previously, many machine learning and DL-based studies have struggled to identify Alzheimer's and dementia stages in the early stages. Due to less helpful information or features, it impacts the performance of the detection models (Billeci et al., 2020).

Currently, identifying MCI in the early stages proves to be a challenging task, mainly when working with limited annotated data samples and extracting detailed feature maps. The MCI stage is a crucial phase in the evolution of AD, occurring between normal cognitive function and the decrease leading to LMCI. LMCI represents a significant decline in both functional and mental abilities. We have developed creative strategies utilizing advanced deep learning and transfer learning models in response to the limited availability of annotated data samples. Our proposed model, Siamese 4D-Alznet, effectively addresses the challenge by extracting detailed feature maps from annotated data samples. Here are the highlights of the proposed work.

- Introduced the Siamese 4D-Alznet, which combines five distinct blocks of CNNs.
- We proposed three custom TL models incorporating frozen and replacing layers.
- Our methods prove 95.07% binary classification performance in terms of accuracy.
- All techniques performed best for NC, EMCI, LMCI, and AD classification.

Related work

The integration of structural and functional connection characteristics in brain research is of great significance, as it plays a crucial role in enhancing the clinical assessment of cognitive impairment. Although it is essential to combine these factors, successfully combining the structural and functional characteristics to understand the complexities of the brain network is still a difficult task. Tackling this difficulty is essential for gaining new understanding of brain function and malfunction, which might have significant consequences for improving diagnostic and therapeutic approaches in the field of cognitive health (Zuo et al., 2023). Furthermore, The highly linked multilayer algorithms' substantial enhancement in binary categorization performance indicates that the CNN is effective in addressing the prevalent issue of class imbalance (Hu et al., 2020). Examining the responses of the feature representations associated with the image makes it possible to investigate the exact regions that contribute to the prediction (Yu et al., 2023). The multilayer computational model is specifically designed to produce a sequence of sub-fund visuals that include relevant local characteristics (S. Wang et al., 2021).

AD studies constantly explore many approaches to predict future states using biomarkers and automated detection. In this context (Amoroso et al., 2018), the authors have outlined a random forest-based approach for feature detection. The model was trained on four distinct classes, but the ML technique yielded a relatively low accuracy score, achieving around a 79% performance rate. The authors employed the CNN Cascade method for automated feature detection. During preprocessing, 397 subjects were included, comprising 100 NC individuals, 93 AD patients, and 204 subjects with MCI, and a categorization accuracy of 93.50% was achieved (Manhua Liu et al., 2018). Researchers employed a hybrid approach, combining data samples from sMRI and DTI, with a primary focus on the region of interest (ROI) of the hippocampus (Lin et al., 2018). The main objective of this article is to forecast the conversion rate from MCI to AD. Initially, they processed the MRI data and registered all the samples. Subsequently, they extracted local patches from the processed data samples to create input samples for the CNN models. Pre-processing involved the utilization of the FreeSurfer tool, which resulted in an 80% performance rate (Vasant et al., 2019).

Moreover, the authors discussed an additional 3D-CNN method applied to early AD detection, utilizing fMRI data samples. This approach involves extracting spatial information from the 4D volume, effectively addressing processing challenges (Wu et al., 2020). The primary goal of this study was to work with ADNI-1 and ADNI-2 datasets and detect MCI and AD. The authors employed 2D and 3D-CNN models, achieving an 89.42% performance in distinguishing NC-AD. A noteworthy contribution of this research was the utilization of ADNI-2 data in conjunction with a 3D-CNN model (Gu et al., 2018). A novel deep CNN-based technique that is more focused on the prediction of mental status assessment (MSA) and AD detection was introduced by the

researchers. They used a total of 331 subjects that belong to the fMRI modality. Transfer learning is a notable ML technique renowned for its capacity to yield superior results even when dealing with limited data samples (Franciotti et al., 2023). Oktavian et al. (2023) proposed an alternative transfer learning model that handles two distinct modalities, MRI and PET. They employed ResNet18 with fine-tuning to classify the three classes of AD. Heising and Angelopoulos (2022) introduced another LENet-5 model for the detection of early MCI. A total of 3312 participants were included in this study, and the BET-2 tool was used for skull stripping and preprocessing the data samples. Two activation functions were employed to identify better performance, resulting in an achieved 84% accuracy.

Odusami et al. (2022) employ two transfer learning models with MRI data. During the experimental phase, the authors combined these two modified models to introduce a hybrid model primarily based on ResNet and DenseNet architectures. This hybrid model achieved a 98.90% accuracy for multiclass classification. Researchers (Pandey et al., 2022) introduced five pre-trained models for the early detection of AD and MCI. The pre-trained models had initially been trained in a different domain and were subsequently fine-tuned using MRI data to obtain classification results. GoogleNet achieved a binary classification accuracy of 96.81%. In their study, authors (Deepa and Chokkalingam, 2022) recommended a customized VGG-16 model for AD detection. They employed the CAT12 (Gaser et al., 2022) tool for pre-processing T1-weighted MRI data to prepare it for input into the customized VGG-16 model. The suggested model achieved an accuracy of approximately 98% by utilizing various optimization functions. Nevertheless, researchers have developed different DL and transfer learning models for AD classification. Researchers utilized MobileNet models based on transfer learning. They improved the classification results, achieving a 96.61% performance by incorporating learnable weighted pooling layers (Xing et al., 2023). In another research study, multiple CNN and RNN models were proposed for analyzing 2D and 3D MRI data. Upon completing the analysis, the final model achieved a classification accuracy of 96.88% (Ebrahimi et al., 2021).

EXPERIMENTAL PROCEDURES

Preprocessing of dataset

The most frequently employed database for early-stage AD detection is the ADNI. Dr. Michael Weiner directed the development of this comprehensive database, which was established through a public–private partnership with a primary focus on utilizing various modalities, including MRI and PET scans, among others (https://adni.loni.usc.edu/data-samples/access-data/). The ADNI team primarily emphasizes the assessment of biological biomarkers and monitoring of physiological changes in AD patients. The ADNI database contains both T1 and T2-weighted MRI scans, although this article utilizes explicitly the T1-weighted MRI modality (Jack et al., 2008). Four categories are employed to facilitate early AD detection: NC, MCI, LMCI, and AD. A total of 310 subjects are distributed across these four classes. Furthermore, demographic details for all participants are provided in Table 1, which displays the mean age for each of the four datasets and the gender distribution within each group. The mean Mini-Mental State Examination (MMSE) score is also included.

Each data sample collected from the database predominantly comes with a NIFTI extension. During the experimental process, these data samples are transformed into 2D slices and converted into PNG or JPEG image formats before being fed into the deep learning model. After data extraction, further preprocessing is necessary to enhance the quality of the scans, thereby enabling the extraction of more valuable features and achieving improved classification results. Numerous tools are available for MRI data preprocessing. In this study, we employed the SPM-12 (Friston et al., 1994) to perform multiple operations aimed at enhancing the quality of the scans. For example, a critical step involves skull stripping, which entails removing the upper portion of the skull from the brain images. Additionally, image registration plays a pivotal role in improving feature visibility. Following this, image normalization is crucial to eliminate minor noise artifacts present in the images and standardize the data to a homogeneous format, thus reducing noise and ensuring the consistent intensity of scans, which facilitates the detection of various brain regions. Finally, segmentation is another vital step in the preprocessing pipeline, wherein the entire MRI dataset is partitioned into white matter, gray matter, and cerebrospinal fluid components.

Proposed Siamese 4D-AlzNet network

In this part, we present the Siamese 4D-AlzNet network for the classification of AD, which has several CNN layers for early identification of MCI. The suggested architecture makes use of four CNNs streams with shared parameters to generate a feature value as an output depicted in Fig. 1. Consider T1-weighted images $\{(x_i, y_i), i = 1, 2, ..., n\}$ containing n feature vectors $x_i \in R^m$, each of size m, and labels $y_i \in \{1, 2, ..., n_1\}$ First, create an initial training set $AD_s = \{(x_i, x_j, x_k, x_l, z_{ij}), (i,j) \in k\}$ including pairs of samples $x_i x_j$ and $x_k x_l$ with associated binary labels $z_{ij} \in \{0, 1\}$ named as NC and AD patients. The parallel execution of four input feature vectors x_i, and have their outputs semantically concatenated and becomes a final feature vector $x_u = \{o_1, o_2, o_3, o_4\}$. After applying a fully connected layer, the resultant output is obtained in the form of $\widehat{y} = \sigma(x_u w_1) w_2$. In addition, the output vector is also shaped as follows $\widehat{y} \in R^{1 \times M}$ where $x_u \in R^{1 \times N}, w_1 \in R^{N \times L}$, and $w_2 \in R^{L \times O}$ is the number of features, L is several hidden units, and O is the output units. σ is an activation function that may be applied to each component of the matrix autonomously. The final classification result from the training set may be separated into two subsets: a comparable or NC with $\widehat{y} = 0$ and a dissimilar or AD set with $\widehat{y} = 0$. The cross-entropy loss is used to optimize the Siamese 4D-AlzNet

Table 1. Comprehensive participant demographic data, including information on subject grouping, age distribution, and MMSE scores. The experimental process involves a total of 310 subjects

Category	NC	MCI	LMCI	AD
Age (±)	73.18 ± 5.56	72.41 ± 4.82	75.84 ± 6.27	78.58 ± 7.61
Subject Size	75	75	80	80
Gender (Male/Female)	45/30	35/40	38/42	46/34
MMSE (±)	28.96 ± 1.01	26.57 ± 1.09	23.97 ± 1.13	22.57 ± 1.05

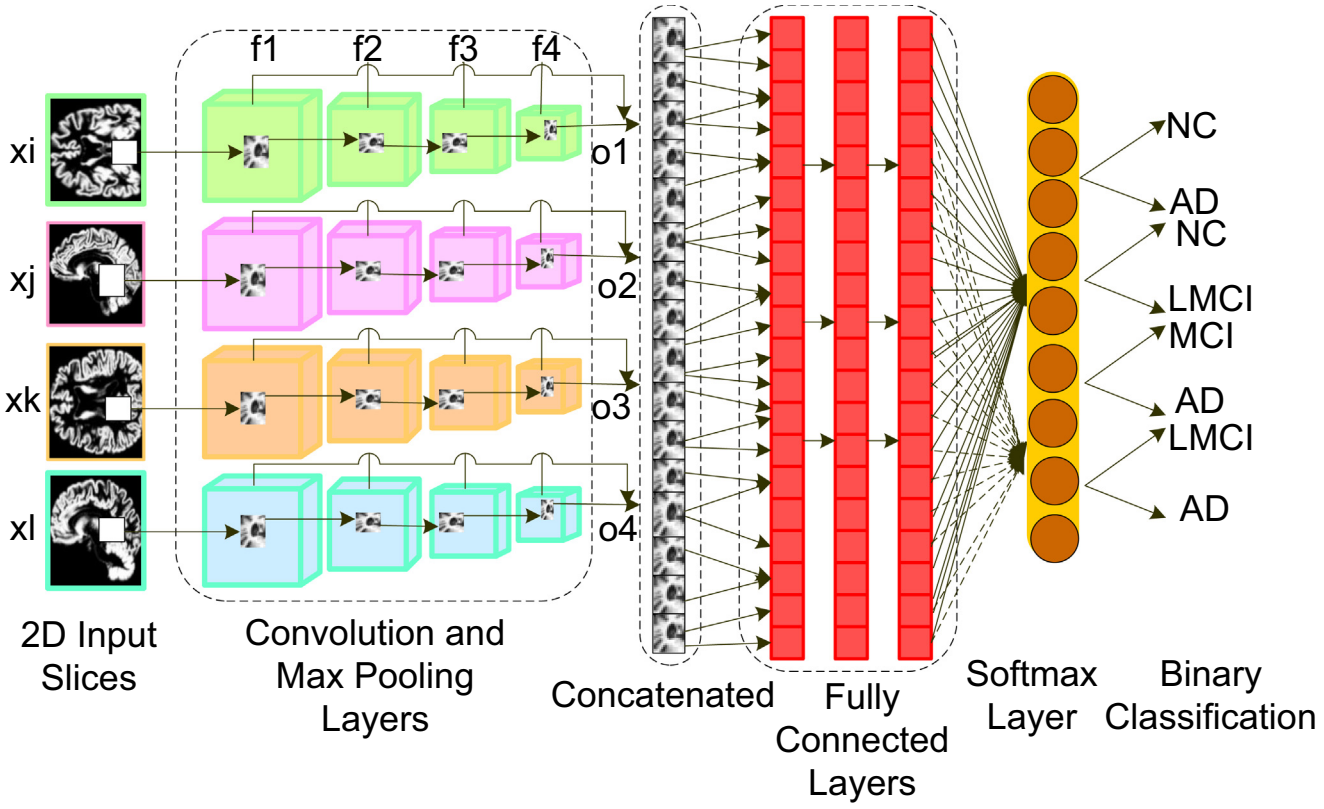

Fig. 1. A systematic diagram of the proposed Siamese 4D-AlzNet architecture consists of four inputs and four CNN streams with multiple flattened outputs. (f1&f2&f3&f4 = flatten output).

network during training, which evaluates the variance among the two probability distributions for given random variables. Binary cross entropy (BCD) is described as:

$$\sum_{i=1}^{c} y_i \cdot \log\left(p\left(\widehat{y}_i\right)\right) + (1-y_i).\log\left(1-p\left(\widehat{y}_i\right)\right) \quad (1)$$

Where, $\widehat{y}_i = 1 \rightarrow \log\left(p\left(\widehat{y}_i\right)\right)$ and $\widehat{y}_i = 0 \rightarrow \log\left(1-p\left(\widehat{y}_i\right)\right)$.

L2 regularization for the proposed model has been applied to prevent over-fitting issues. The main challenge of L2 regularization is described in Eq. (2), W a matrix containing the parameters of the neural network; λ is a hyper-parameter that regulates the degree of regularization.

$$\lambda \sum_{i,j,l} \left(W_{ij}^{l}\right)^2 \quad (2)$$

Convolutional neural network

This study employs CNNs that include Convolutional (Conv), pooling, and fully connected (FC) layers. CNN depends on three architectural concepts: sharing weights, localized receptive fields, and temporal sub-sampling to achieve invariance in rotation, translation, and scaling (Mehmood et al., 2022). Here, the Siamese 4D-AlzNet network is comprised of five blocks of Conv layers, and four max-pooling layers (Pooling-1, Pooling-2, Pooling-3, and Pooling-4). Here, $x_i x_j$, x_k, x_l are the input images with dimensions of 224 × 224 that have been normalized and aligned, mainly given to block-1. Following that, every single neuron in the hidden layer receives input from a group of units situated within a relatively small neighborhood of the preceding layer. The output of each convolution block is kept in a vector called flatten and passed to the max-pooling layer for further sub-sampling of the feature map. As a result, it can be written as:

$$h_o = f\left(x_{(i,j,k,l)} * w_o + b_o\right) \tag{3}$$

Eq. (3), $x_{(i,j,k,l)}$ is an input tensor that is convolved with a kernel of weights w, then a bias term b is added, and finally the output is passed via a non-linearity to the current hidden layer h_o. The improved form of the convolutional formulae, shown in Eq. (4), is the input of the feature map for the pooling layer, w^l_{mo} denote as a weight vector connecting to feature map of the output layer, and b^l_{mo} as a bias paired with the input signal. As the outcome, the output feature map in a layer is created as follows:

$$h^l_o = f\left(\sum_m x^{l-1}_{(i,j,k,l)m} * w^l_{mo} + b^l_{mo}\right) \tag{4}$$

Moreover, '$*$' stands for the convolutional operations, and f is the activation function of a rectified linear unit (ReLU) in the hidden layer, as determined by $f\left(x_{i,j,k,l}\right) = \max\left(0, x_{i,j,k,l}\right)$, and Siamese 4D-AlzNet networks label predictions are made using softmax. The ReLU activation function offers non-linearity in the extraction of features, which is far more useful for training than the conventional and typical activation functions such as hyperbolic tangent (tanh) and sigmoid. All blocks convolution phases in the convolutional layers are similar to block-1 (Conv1), except for the size and length of the convolutional filters. In CNNs, two pooling strategies are typically utilized. Local pooling is the initial technique for displaying feature maps, which gathers data from relatively tiny local regions (like 3 × 3). The most significant value of the region is then chosen and placed in the output's relevant pixel position. Every feature vector from the Conv block is passed to the Pooling (1–4) layers created using the max pooling sub-sampling technique and applied to the relevant feature vectors in the preceding layer. The mathematical illustration is shown in Eq. (5), where the filter height and width are the coordinates, and h^l_o is the output of block-1 (*i.e.*, two convolutional layers). The benefit of max-pooling is to build a layered framework for feature extraction, and it reduces the spatial size of every feature vector as well as the number of calculations in the network.

$$\widetilde{h}^l_o(a,b) = \max h^l_o(a+u-1, b+v-1) \tag{5}$$

The Pooling layer result is saved as a separate feature vector and also sent to the next block of convolutions. This process will be repeated until all five blocks have been completed. The resulting vector of all convolution and max-pooling blocks, as well as all pre-pooling feature vectors, are now concatenated. The last layer of the model is the fully connected layer (FC), which works as a stacked linear classifier. The Softmax classifier will be given the feature maps with constant dimensions that are the outcome of the preceding layers. The classifier output computes the probabilities of the AD classes for every input image, with the most outstanding value being the predicted AD class. Fig. 2 depicts the overall process of the proposed framework, and Table 2 shown the properties of the model.

Evaluation metrics

Different assessment measures are used to assess the classification results produced using the Siamese 4D-AlzNet architecture, such as Accuracy, Recall, Precision, and F1-Score, as shown in Eqs. (6–9). These measurements provide essential context for understanding the diagnostic accuracy of the model. Hence, recall describes the model sensitivity and reveals the percentage of correctly diagnosed patients that is crucial for accurate disease detection. On the other hand, precision measures how many times a model accurately predicts a good outcome. For the AD experimental dataset, a model must eliminate false positives.

$$Accuracy = \frac{TP + TN}{TP + TN + FP + FN} \tag{6}$$

$$F1 - Score = \frac{2 \times precision \times recall}{precision + recall} \tag{7}$$

$$\text{Re}call = \frac{TP}{TP + FN} \tag{8}$$

$$\text{Pre}cisoion = \frac{TP}{TP + FP} \tag{9}$$

Experimental results of the proposed model

Two strategies are used to classify AD medical images. The first technique is based on conventional CNN frameworks that work with brain MRI data using 2D convolution filters. The designs of parallel CNN blocks comprised of convolutional and pooling layers are created from scratch. The second approach makes use of the pre-trained weights by using transfer learning methods for medical image classification.

The proposed algorithm is structured around five distinct blocks of Convolutional Neural Networks (CNNs), each featuring a varying number of convolutional layers and convolution filter sizes. An initial max-pooling operation is applied to the entire input data sample to initiate the processing. Subsequently, this pooled input is directed through each of the five blocks for further refinement. Block 1 comprises two convolutional layers, each utilizing a 3x3 kernel and twelve convolutional filters. L2 regularization and ReLU activation functions are applied within these convolution layers, and batch normalization is inserted between these layers. The first intermediate output from Block-1 is obtained by flattening the output and connecting it to a sigmoid-dense block. Each block retains its feature map as an output. Block-2 and Block-3 each contain four convolutional layers with the same kernel size and number of convolutional filters as Block-1. Block-4 and Block-5 encompass eight convolutional layers, again maintaining the same kernel size and number of convolutional filters as Block-1. In the context of Siamese 4D-AlzNet, these five blocks concurrently process the input data in four parallel streams. Following this, all the feature maps these blocks generate are concatenated and subsequently forwarded

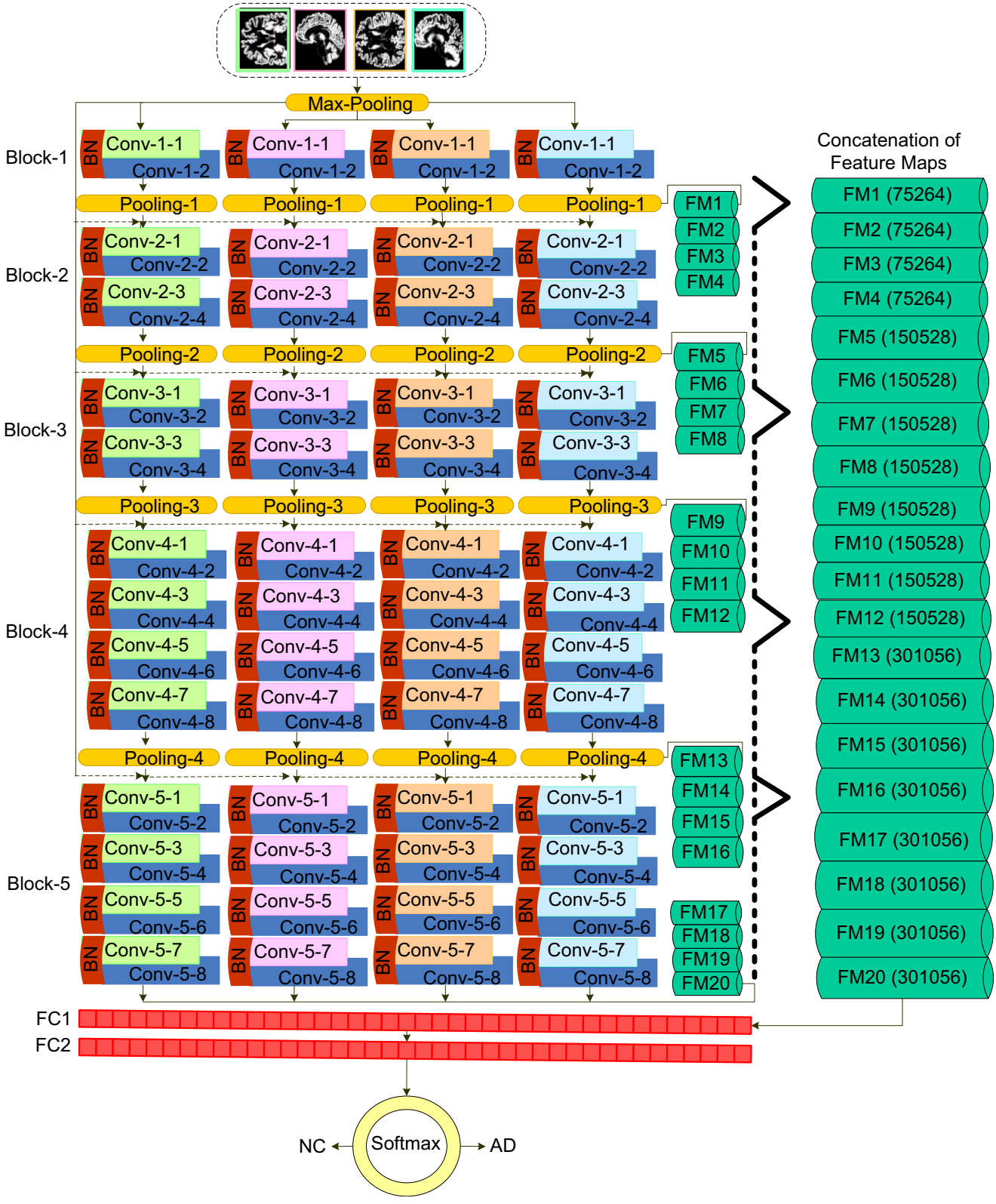

Fig. 2. Illustrates the stepwise progression of block-wise convolutional and pooling layers within the Siamese 4D-AlzNet network. This network consists of five blocks of CNN, each featuring varying numbers of convolutional layers. The first block includes two convolutional layers, while blocks two and three comprise convolutional layers, and blocks four and five consist of eight convolutional layers. (Abbreviations: FM = Feature Map; FC1 & FC2 = Fully Connected; Conv = Convolution).

Fig. 3. Loss was tracked throughout the 100 epochs of training for the binary classification tasks involving MCI-AD (**A**), NC-AD (**B**), and NC-MCI (**C**) classes.

Table 2. Properties of the proposed model in terms of several layers, feature map, and trainable parameters (CL = convolutional layers, BN = Batch Normalization, MP = Maxpooling)

No. of bocks	No. of layers	Feature map	Trainable parameters
Block 1	2 (CL + BN) + MP each sub-block1	FM1, FM2, FM3, FM4	301,056
Block 2	4 (CL + BN) + MP each sub-block2	FM5, FM6, FM7, FM8	602,112
Block 3	4 (CL + BN) + MP each sub-block3	FM9, FM10, FM11, FM12	602,112
Block 4	4 (CL + BN) + MP each sub-block4	FM13, FM14, FM15, FM16	1,204,224
Block 5	4 (CL + BN) + MP each sub-block5	FM17, FM18, FM19, FM20	1,204,224

to the fully connected layers FC1 and FC2. Using these feature maps, a Softmax layer is employed to classify AD stages. The primary goal of the proposed Siamese neural network technique is to mitigate reliance on extensive datasets. This approach effectively addresses the challenge by extracting detailed feature maps from a limited annotated data sample set, leading to improved results.

Moreover, this study employed three transfer learning techniques: customized AlexNet, Frozen-VGG-16, and Frozen-VGG-19 models with pre-trained weights for AD image classification. Low-level features are obtained in the initial layers of pre-trained models, while class-specific features reside in the final layers. The primary focus is training the network for a 2D Alzheimer dataset by replacing the class-specific layers. Specifically, the first three layers of the AlexNet model were transferred and replaced with new layers. Similarly, for the Frozen-VGG-16 and VGG-19 networks, the last four and five convolutional layers have been frozen, respectively. The FC layers parameters were carefully considered, including weight-learning factor, bias-learning factor, and output size. The output size of this fully connected layer matched the number of output classes, with the weight-learning factor controlling the learning rate for layer weights and a separate bias-learning parameter controlling the learning rate for layer biases.

The training began with an initial learning rate of 0.0001, with the Adam optimizer facilitating dynamic learning rate modifications. Training sessions were conducted with a batch size of 32, utilizing the computing capabilities of a Precision 7670 Workstation equipped with an NVIDIA RTX A4500 64 GB GDDR6 and a 12e generation Intel® CoreTM i9-12850HX, vPro®. An early stop mechanism has been added to the training routine as an avoidance against over-fitting issues. Various hyper-parameters for the proposed model and pre-trained techniques were established using the hit-and-trial method. During the training procedure, 100 epochs were utilized with the binary cross-entropy loss function, and data distribution details are shown in Table 3.

Performance evaluation for NC-AD

This section describes the simulation results of the proposed model for five binary classifications. In Fig. 4, we present a comprehensive assessment of the performance of these models through confusion matrices. These matrices illuminate the accuracy and effectiveness of each model in distinguishing between AD and NC cases.

In the case of the Siamese 4D-AlzNet model, it impressively classified 692 scans as AD and 448 as NC, demonstrating its robust capability in correctly identifying Alzheimer's cases. Similarly, the frozen VGG-16 model exhibited noteworthy performance by accurately predicting 650 AD and 419 NC images.

Table 3. The binary dataset has been partitioned into four distinct classes, to create separate sets of images for training and testing. To achieve this partitioning, 80% of the dataset has been allocated for the training phase, while the remaining 20% has been designated for testing purposes

Dataset Classes	No. of images (Training)	No. of images (Testing)	No. of images Total
NC Subjects	2016	504	2520
MCI Subjects	1596	399	1995
LMCI Subjects	2780	695	3475
AD Subjects	2780	695	3475

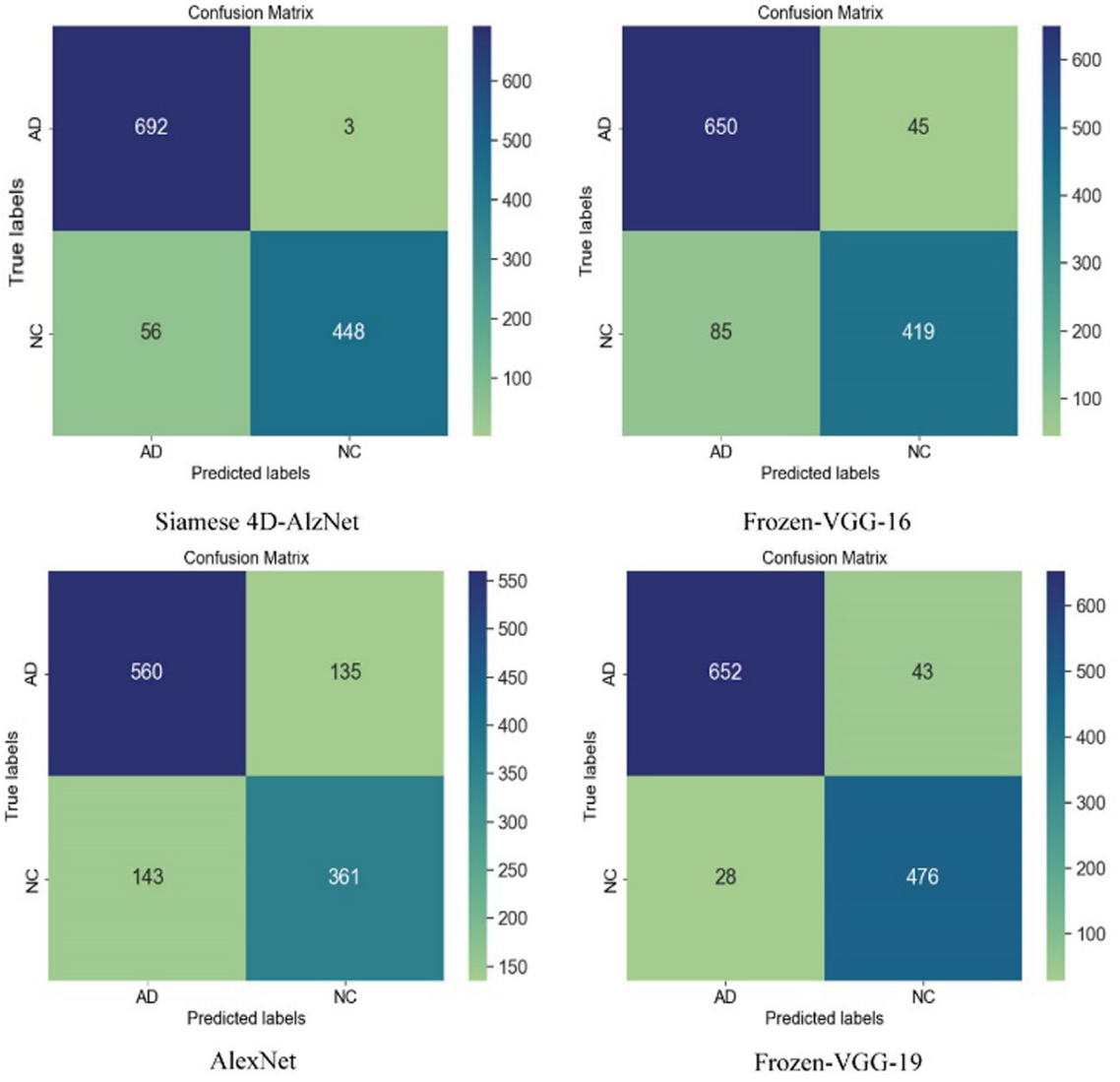

Fig. 4. Confusion matrix of Siamese 4D-AlzNet and pre-trained techniques for binary class NC and AD.

Furthermore, the Frozen VGG-19 model also shows remarkable performance in classification, correctly indicating 652 test images. A comprehensive summary of the performance metrics for all proposed models is presented in Table 4. It becomes evident that the Siamese 4D-AlzNet model stands out as the top performer, achieving an impressive accuracy rate of 95.07% and a remarkable recall rate of 95.90%. This emphasizes its exceptional ability to distinguish between AD and NC cases accurately. The frozen VGG-19 model obtained the second-best result for NC-AD classification, achieving a praiseworthy accuracy rate of 94.08%. Furthermore, training loss for three binary classes also shown in Fig. 3.

Performance evaluation for NC-LMCI

The classification score for NC-LMCI classification of all proposed models are illustrated in Table 5, where the Frozen VGG-16 based approach attained (96.91% accuracy, precision of 77.98%, and F1-score 87.34%), similarly Frozen VGG-19 (accuracy of 94.58%, precision

Table 4. Proposed Siamese 4D-AlzNet and three customized models performance w.r.t accuracy, precision, F1-Score, and recall for the classification of NC-AD

Metrics	Siamese 4D-AlzNet	Frozen VGG-16	AlexNet	Frozen VGG-19
Accuracy	95.07	89.16	76.81	94.08
Precision	99.56	93.52	80.57	93.81
F1-Score	95.90	90.90	79.02	94.83
Recall	92.51	88.43	79.65	95.88

Table 5. Proposed Siamese 4D-AlzNet and three customized models performance w.r.t accuracy, precision, F1-Score, and recall for the classification of NC-LMCI

Metrics	Siamese 4D-AlzNet	Frozen VGG-16	AlexNet	Frozen VGG-19
Accuracy	96.75	86.91	89.15	94.58
Precision	98.56	77.98	83.16	91.22
F1-Score	97.22	87.34	89.88	95.12
Recall	95.93	99.26	97.80	99.37

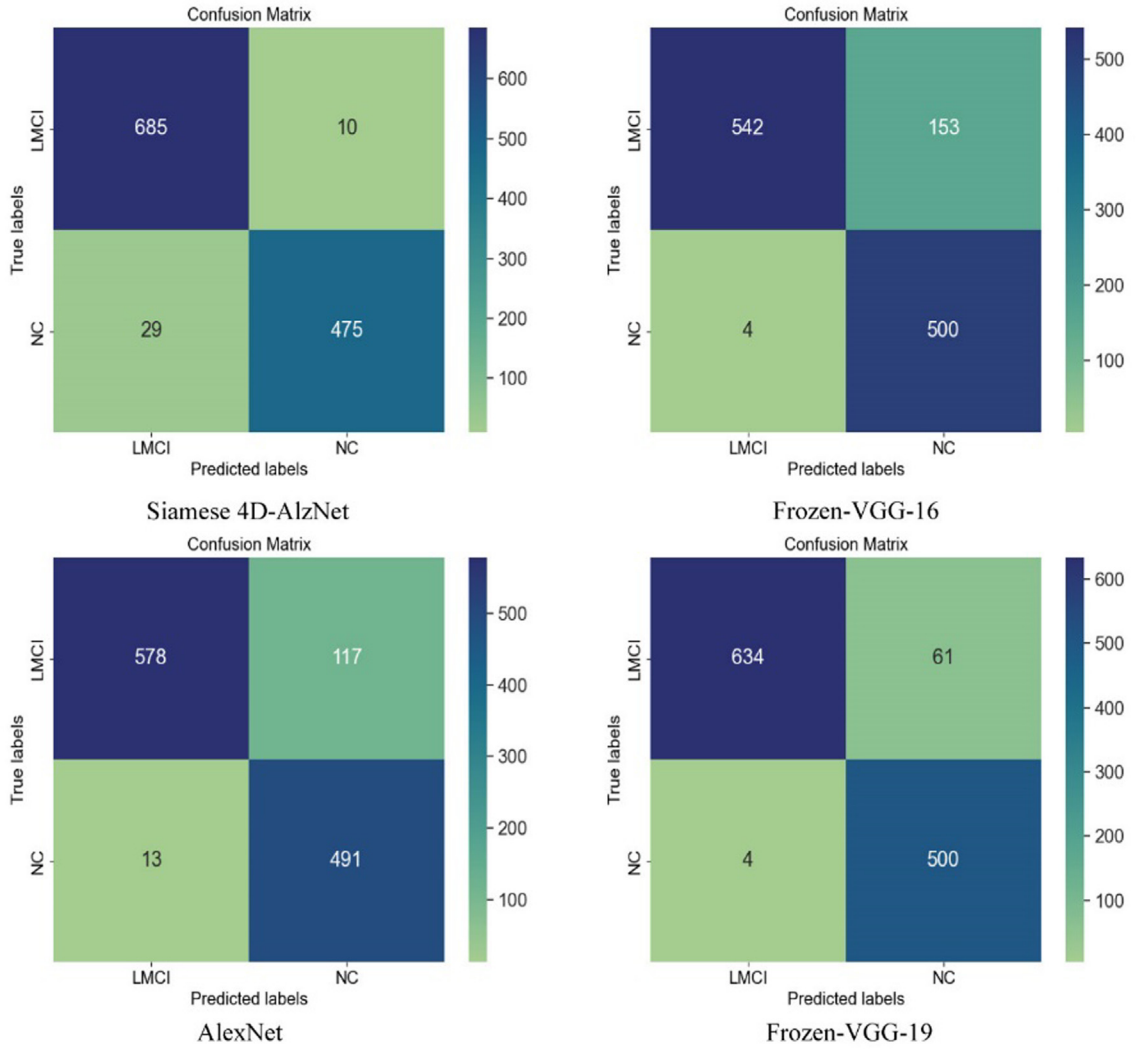

Fig. 5. Confusion matrix of Siamese 4D-AlzNet and pre-trained techniques for binary class NC and LMCI.

91.22%, F1-Score 95.12%, and Recall 99.37%). Finally, Siamese 4D-AlzNet produced the best result (accuracy 96.75%, precision 98.56%, F1-Score 97.22%, and Recall 95.93%). The results of this study are shown in Fig. 5 as a confusion matrix based on the optimum performance of each model.

Performance evaluation for NC-MCI

Table 6 visually represents the results obtained from our comprehensive metric evaluation for binary classification. We have observed substantial improvements in the performance of these algorithms when applied to the NC-MCI classification task. Mainly, customizing the AlexNet architecture has led to a gradual increase in performance compared to the previous binary classification task of NC-AD. However, it is worth highlighting that the most outstanding performance is attributed to the Siamese 4D-AlzNet model, boasting an exceptional accuracy rate of 96.82%.

In comparison, the Siamese 4D-AlzNet model shares a similar level of performance with the Frozen VGG-19 model, although it outperforms it by a margin of 0.84%. Frozen VGG-16, for instance, achieved impressive results, with a precision score of 91.47%, a recall rate of

Table 6. Proposed Siamese 4D-AlzNet and three customized models performance w.r.t accuracy, precision, F1-Score, and recall for the classification of NC-MCI

Metrics	Siamese 4D-AlzNet	Frozen-VGG-16	AlexNet	Frozen-VGG-19
Accuracy	96.82	91.88	88.27	95.98
Precision	96.49	91.47	85.71	94.48
F1-Score	94.24	91.58	88.13	96.04
Recall	92.1	91.7	90.71	97.66

91.70%, and an F1 score of 91.47%. These metrics emphasize the models ability to effectively and accurately classify NC and MCI cases. We conducted a detailed analysis using confusion matrices for a more comprehensive understanding of the classification algorithm performance. These matrices provide insights into the variation in true positives and negatives, as depicted in Fig. 6.

Performance evaluation for MCI-AD

The results demonstrate the superior performance of the proposed Siamese 4D-AlzNet model on the ADNI dataset for MCI-AD, achieving an impressive accuracy rate of 95.43%, as described in Table 7. This accuracy surpasses that of other pertained models by a substantial margin, with differences of 0.55%, 4.48%, and 14.99% for Frozen-VGG-19, Frozen-VGG-16, and

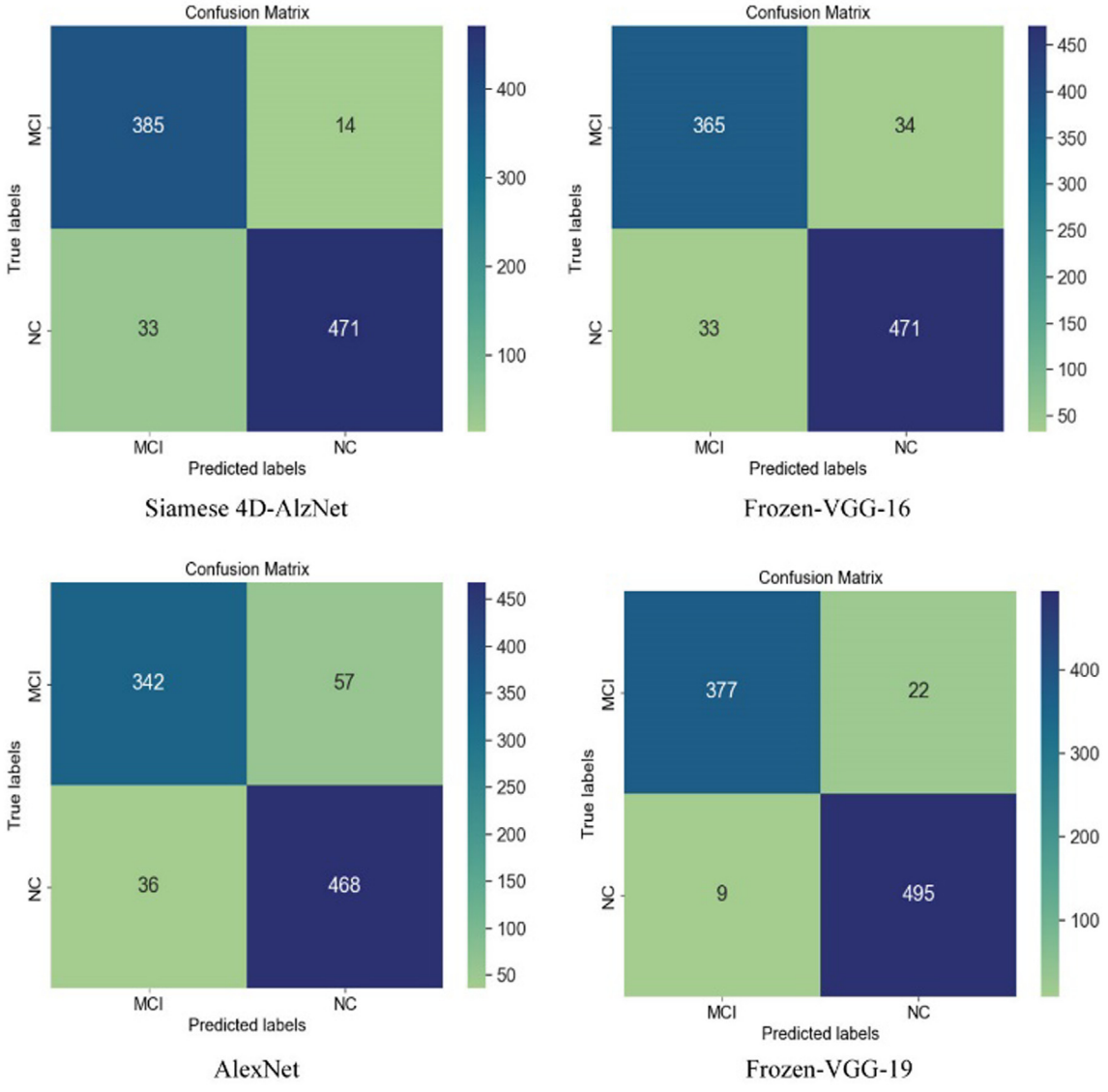

Fig. 6. Confusion matrix of proposed Siamese 4D-AlzNet and pre-trained techniques for binary class NC and MCI.

Table 7. Proposed Siamese 4D-AlzNet and three customized models performance w.r.t accuracy, precision, F1-Score, and recall for the classification of MCI-AD

Metrics	Siamese 4D-AlzNet	Frozen-VGG-16	AlexNet	Frozen-VGG-19
Accuracy	95.43	80.44	90.95	94.88
Precision	98.12	81.29	97.12	98.41
F1-Score	96.45	84.07	93.16	96.06
Recall	94.85	87.05	89.52	93.82

customized AlexNet, respectively, in terms of MCI-AD classification accuracy rate. Furthermore, the Siamese 4D-AlzNet model also excelled in the F1-Score, a crucial aggregate measure that combines precision and sensitivity. It achieved an outstanding F1-Score of 96.45%. This high F1-Score indicates the model's ability to balance precision and sensitivity effectively, which is particularly important in medical applications like AD diagnosis, as depicted in Fig. 7.

Performance evaluation for LMCI-AD

In Table 8, we present the classification scores for the LMCI-AD classification task across various proposed models. Notably, the AlexNet-based approach achieved an accuracy of 77.61%, demonstrating its competence in distinguishing between LMCI and AD. Furthermore, this model exhibited a precision of 95.25%, an F1-Score of 84.38%, and a recall rate of 75.74%. Similarly, the Frozen VGG-19 model also delivered better results with

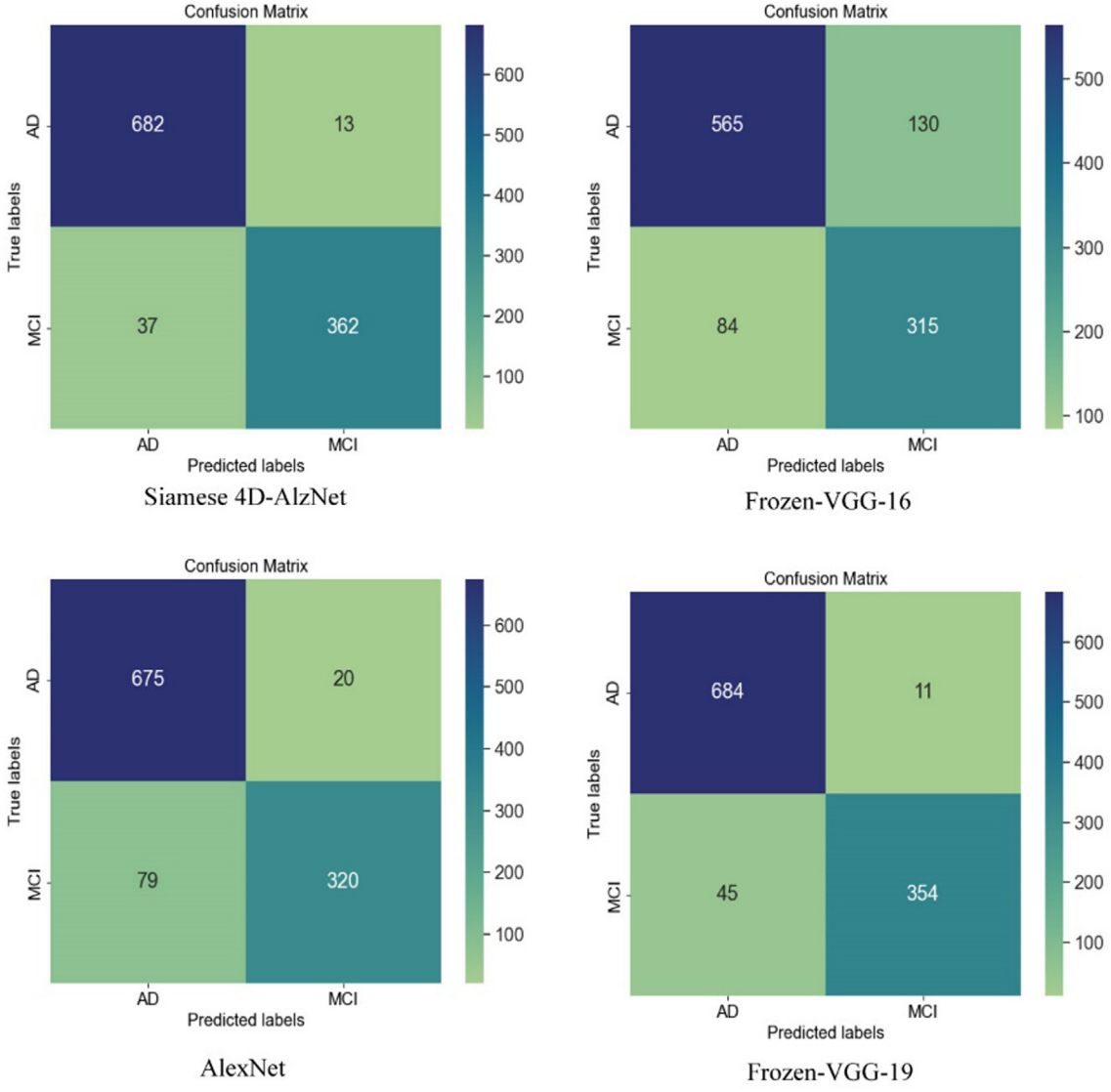

Fig. 7. Confusion matrix of Siamese 4D-AlzNet and pre-trained techniques for binary class MCI and AD.

Table 8. Proposed Siamese 4D-AlzNet and three customized models performance w.r.t accuracy, precision, F1-Score, and recall for the classification of LMCI-AD

Metrics	Siamese 4D-AlzNet	Frozen-VGG-16	AlexNet	Frozen-VGG-19
Accuracy	79.16	78.34	77.61	80.70
Precision	98.56	99.28	95.25	96.97
F1-Score	86.05	85.46	84.38	86.45
Recall	76.36	74.89	75.74	78.01

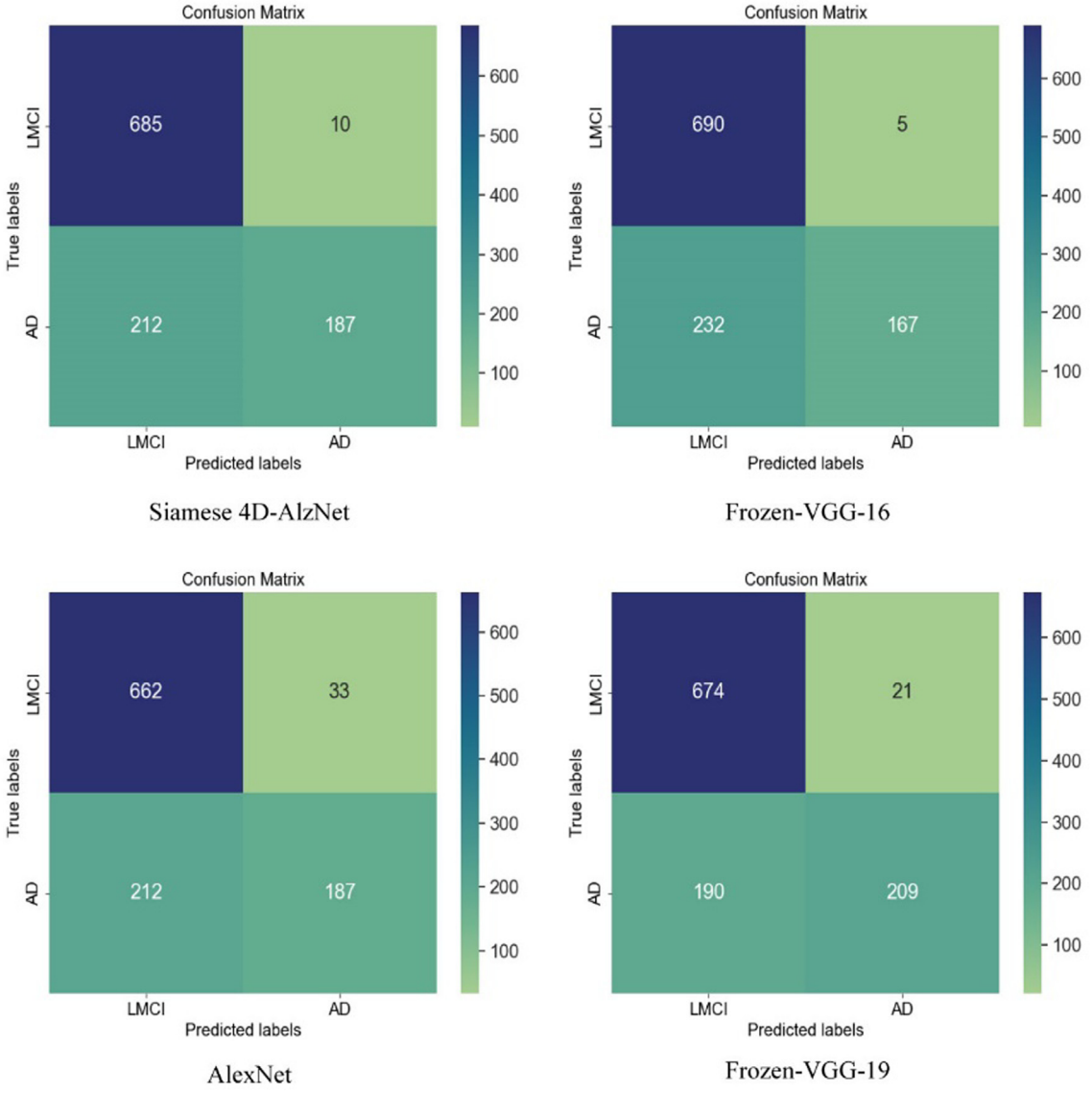

Fig. 8. Confusion matrix of Siamese-4D-AlexNet and pre-trained techniques for binary class LMCI - AD.

an accuracy of 80.70%. This model showed impressive precision (96.97%), an F1-Score of 86.45%, and a recall rate of 78.01%. On the other hand, the Frozen-VGG-16 model, while still achieving an accuracy of 78.34%, demonstrated relatively lower performance than the above-mentioned models. Its precision stood at 85.46%, the F1-Score at 85.46%, and recall at 74.89%. Fig. 8 is the representation of the confusion matrix of LMCI-AD binary classification.

Comparison of Siamese 4D-AlzNet with customized AlexNet, Frozen-VGG-16, and Frozen-VGG-19 models

Fig. 9 (A, B, C, and D) shows the relative significance of the five binary classes based on its accuracy and F1-Score performance across various techniques. The comparison analysis of the NC class with AD, LMCI, and MCI in A & B subfigures depicts the highest accuracy/F1-Score of NC-LMCI and NC-MCI classes over the NC-AD class. Similarly, the MCI-AD class has

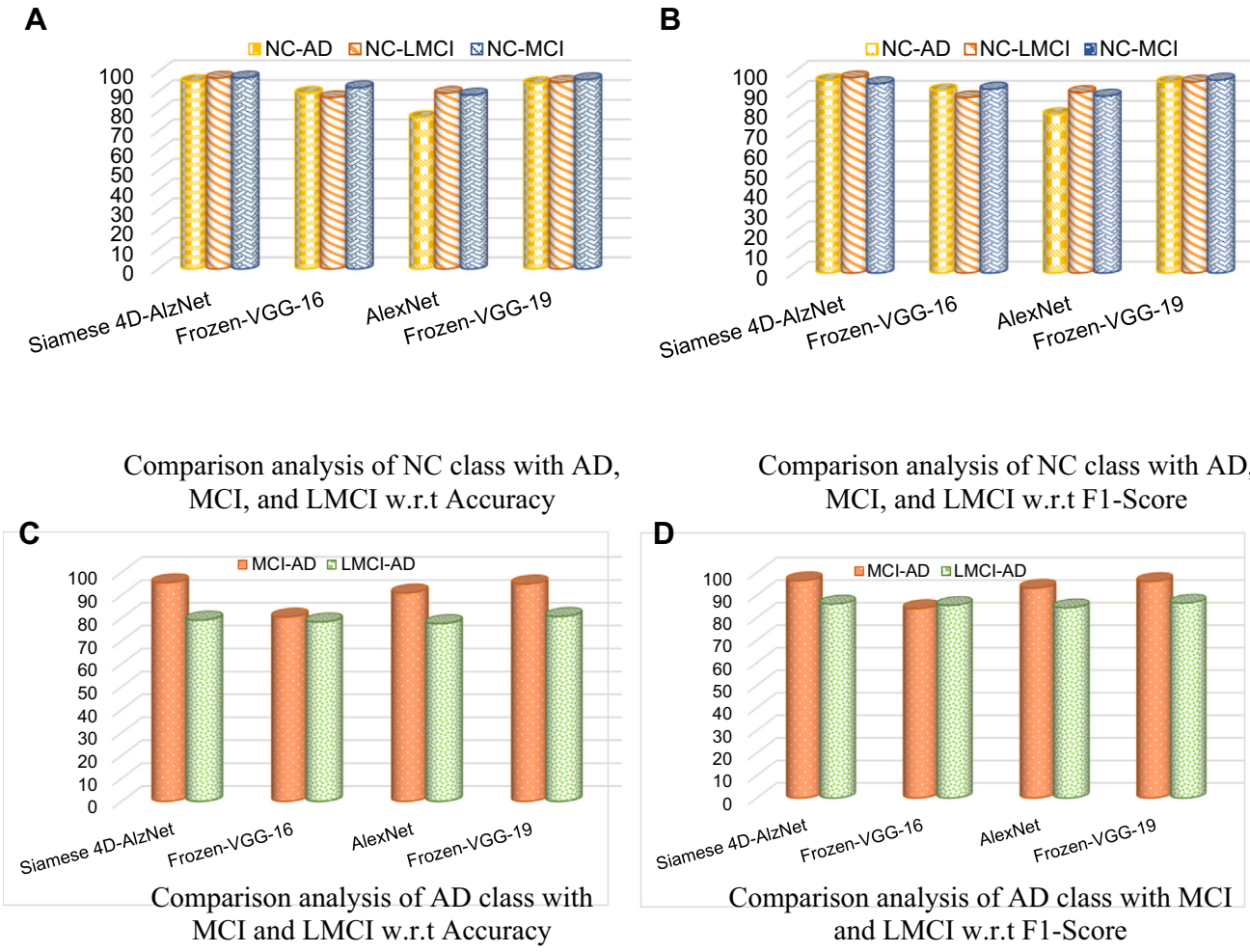

Fig. 9. Bar charts performance evaluation of five binary classes (**A-D**) in terms of accuracy and F1-Score.

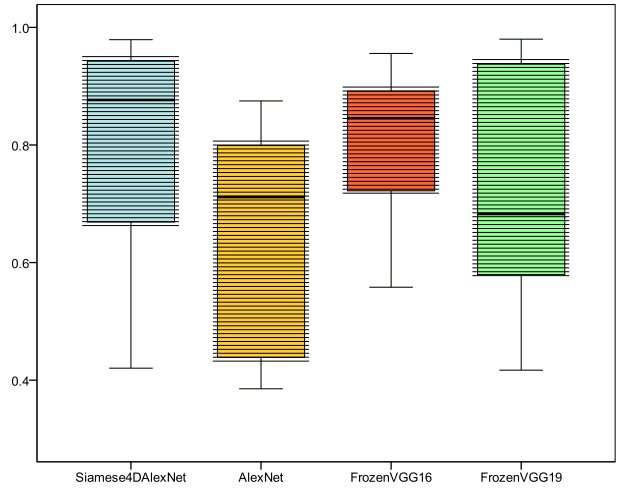

Fig. 10. Box plot comparison analysis of proposed and pre-trained models for NC-AD binary classification in terms of accuracy.

the highest accuracy and F1-Score value evaluated by Siamese 4D-AlzNet than the LMCI-AD binary class among all techniques.

To further evaluate the performance of the proposed Siamese 4D-AlzNet and pre-trained models in terms of accuracy across epochs, Fig. 10 displays a comparative box plot. The Siamese 4D-AlzNet framework consistently achieves 70% and 95% accuracy. In contrast, the pre-trained models exhibit accuracies ranging from 50% to 85%, 70% to 85%, and 55% to 90% on different epochs, respectively.

Additionally, to evaluate the performance of the suggested and trained models for two binary classes, MCI and LMCI with AD, each having distinct precision and recall values, were used for the experiment. The four models are objectively compared and assessed in the form of a comparison bar chart in Fig. 11. The proposed Siamese 4D-AlzNet model showed the exact binary classification results with a precession of 98.12% and 94.85% precision, recall, respectively, for MCI-AD class as compared to LMCI-AD. The precision of the Frozen-VGG-19 model was 98.41%, with the recall value significantly decreased, scoring 93.82%, which changed the classification performance. Overall, while performance is significantly affected by a single lowering of the precision/recall values, it is clear that model prediction performance rapidly declines with further reductions.

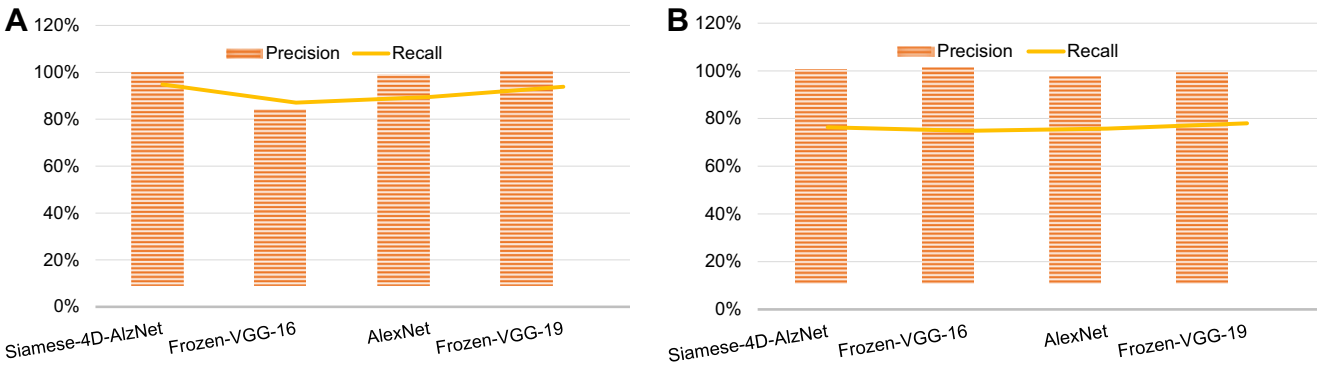

Fig. 11. Binary classification precision (orange) and recall (yellow) in percentage estimation among four models for MCI-AD and LMCI-AD are shown in (**A**) and (**B**), respectively.

DISCUSSION

In this section of our research paper, we critically discuss the methodologies employed for feature extraction and classification in AD identification using MRI data. We explore the significance of deep learning and TL algorithms. However, it is important to note that the effectiveness of these methods often depends on the quality of previously handcrafted features and dimensionality reduction techniques, which may not always yield optimal results in feature extraction. Deep learning, particularly CNNs, primarily relies on gradient-based evaluation metrics to guide feature selection (C. F. Liu et al., 2019a). The choice of hyper-parameters and network architecture, including the number of layers and neurons, directly impacts the classification performance. Therefore, the selection of appropriate parameters is crucial for achieving accurate results in AD detection (H. Wang et al., 2019).

In this article, we introduce a new approach called Siamese 4D-AlzNet, designed with the primary goal of early detection and identification of MCI. Early detection is imperative as it provides an opportunity for intervention and treatment before the condition progresses to the advanced stages of AD. The siamese 4D-AlzNet approach is rooted in the fundamental principles of deep learning. Our model relies on comprehensive feature information extracted from MRI images, and architecture includes four distinct pathways. Within each pathway, multiple CNN blocks are implemented, generating multiple outputs. The inclusion of multiple outputs facilitates immediate feedback during the early evaluation of error functions, enhancing the model's ability to adapt and learn effectively. Dense layers are utilized in each block, connecting to all layers within the same block. After the outputs from the four pathways are extracted, these outputs are associated and connected to the final classifier layer for AD classification. In addition to our Siamese 4D-AlzNet model, we also explore the performance of Frozen VGG-19 and Frozen VGG-16 architectures with certain layers frozen and customized pre-train AlexNet.

We have comprehensively compared the findings from our proposed models, as detailed in Tables 9 and 10. In Table 9, we specifically focused on evaluating the performance of the binary class NC-AD. In this context, Ahmed et al. (2019) reported a maximum accuracy of 85.55%, which was achieved through an ensemble classifier. Their approach also yielded commendable precision (85.66%) and a recall score of 85.52%. Similarly, Hajamohideen et al. (2023) achieved a 91.83% accuracy for the classification of NC-AD.

Comparatively, our Siamese-4D-AlzNet demonstrated a substantial performance improvement when contrasted with other state-of-the-art techniques, showcasing impressive gains of 9.52%, 3.24%, 5.87%, 7.86%, and 8.87% in terms of accuracy. Furthermore, the frozen VGG-19 model also delivered noteworthy results, with accuracy improvements of 8.53%, 2.25%, 4.88%, and 6.87%, respectively. These results underscore the efficacy and superiority of our proposed Siamese-4D-AlzNet model and the frozen VGG-19 model in the classification of NC-AD. The substantial enhancements in accuracy achieved by our models demonstrate their potential to advance the state of the art in the early diagnosis and treatment of AD.

Table 10 presents a comparative analysis of our binary classification models for MCI-AD and other techniques. Notably, Lin et al. introduced a supervised CNN-based classification framework dedicated to the early detection of MCI, achieving an impressive accuracy score of 81.40% with a recall rate of 89.61%. Similarly, another study proposed a 2D-CNN model that delivered compelling results, boasting an 83.30% accuracy rate, 78.60% precision, and an 84.60% recall rate. Notably, our proposed models have shown remarkable improvement in performance, consistently enhancing accuracy by a significant margin, falling within the range of 4–9%. This enhanced accuracy signifies the robustness and effectiveness of our approach in distinguishing MCI from AD. These findings suggest that our models have the potential to provide more reliable and accurate results, which can be invaluable in the early diagnosis and intervention of cognitive disorders.

Overall, our research demonstrates the potential of deep learning techniques and the Siamese-4D-AlzNet model, particularly for early detection of MCI, a crucial step in Alzheimer's disease management and

Table 9. I proposed a comparison of models with other state-of-the-art models in terms of accuracy, precision, and recall for the classification of NC-AD. It achieved the highest accuracy rate, 95.07%

Methods	Dataset	Modality	Accuracy (%)	Precision (%)	Recall (%)
Ensemble Classifier (Ahmed et al., 2019)	ADNI	MRI	85.55	85.66	85.52
Siamese CNN (Hajamohideen et al., 2023)	ADNI	MRI	91.83	–	91.79
ResRepANet (Chen et al., 2022)	ADNI	MRI	89.20	–	90.30
CNN (Tinauer et al., 2022)	ADNI	MRI	87.21	84.38	94.70
Hybrid CNN (Sethi et al., 2022)	ADNI	MRI	86.20	–	–
CNN (Faisal and Kwon, 2022)	ADNI	MRI	97	–	98.40
CNN (Ieracitano et al., 2019)	ADNI	MRI	92.95	91.02	95.30
Ensemble (Ahmed et al., 2019)	ADNI	MRI	85.55	85.43	85.57
Frozen VGG-16	ADNI	MRI	89.16	93.52	88.43
Frozen VGG-19	ADNI	MRI	94.08	93.81	95.88
AlexNet	ADNI	MRI	76.81	80.57	79.65
Siamese 4D-AlzNet	ADNI	MRI	**95.07**	**99.56**	**92.51**

Table 10. Proposed models comparison with other state-of-the-art models in terms of accuracy, precision, and Recall for the classification of MCI-AD. It achieved the highest accuracy rate of 95.43%

Methods	Dataset	Modality	Accuracy (%)	Precision (%)	Recall (%)
CNN (Lin et al., 2018)	ADNI	MRI	81.40	–	89.61
Hybrid CNN (Sethi et al., 2022)	ADNI	MRI	84.90	–	–
CNN (Heising and Angelopoulos, 2022)	ADNI	MRI	73.50	72.80	89.40
2D CNN (Park et al., 2023)	ADNI	MRI	83.30	78.60	84.60
CNN (Basaia et al., 2019)	ADNI	MRI	85.90	–	83.60
CNN (Carcagnì et al., 2023)	ADNI	MRI	71.12	–	–
CNN (Ieracitano et al., 2019)	ADNI	MRI	84.62	84.32	85.04
Frozen VGG-16	ADNI	MRI	80.44	81.29	87.05
Frozen VGG-19	ADNI	MRI	94.88	98.41	93.82
Customized-Alexnet	ADNI	MRI	90.95	97.12	89.52
Siamese-4D-AlzNet	ADNI	MRI	**95.43**	**98.12**	**94.85**

intervention. The methodology presented in this article contributes to the ongoing efforts to improve the accuracy and timeliness of Alzheimer's disease diagnosis and, ultimately, patient care. The ADNI dataset and MRI modality stand out as the primary options for AD classification. Despite their widespread use, effectively managing the entirety of the neuroimaging modality presents a significant challenge for researchers actively engaged in this field. The limitation of this work to not handle multimodality data. Addressing the persistent obstacle of handling complex neuroimaging data in future work will involve incorporating annotated data samples to tackle the multimodality data issue. Additionally, introducing a patch-based technique may enhance results when working with multimodality data samples, offering a potential avenue for improvement in the classification process.

The Siamese 4D-AlzNet framework has been presented in this research as a means of early detection for MCI. The main objective is gradually acquiring knowledge from low-level to high-level feature maps by utilizing a CNN architecture composed of five unique modules. The feature maps that arise from the concurrent processing of input data by these five blocks via four parallel streams are combined and forwarded to the fully connected layers FC1 and FC2. We also introduced three customized transfer learning-based models by replacing and freezing specific layers. A set of experiments has been performed on a dataset consisting of four distinct classes: NC, MCI, Late MCI (LMCI), and AD, all of which were preprocessed before their extraction from the ADNI database. Our results demonstrated the robust classification performance of Siamese 4D-AlzNet across five pairs of binary classes. Our customized transfer learning models, specifically the frozen-VGG-19, exhibited superior performance in brain disease classification compared to alternative methods. In conclusion, the performance of the Siamese 4D-AlzNet framework we have proposed for the early detection of MCI is encouraging. This study makes a significant intellectual contribution to the domain of brain disease diagnosis by potentially assisting in the prompt detection of individuals susceptible to developing mild cognitive impairment.

CONFLICTS OF INTEREST

The authors declare no conflict of interest.

ACKNOWLEDGEMENT

This work was funded by the National Natural Science Foundation of China NSFC62272419, U22A20102, Natural Science Foundation of Zhejiang Province ZJNSFLZ22F020010, and Zhejiang Normal University Research Fund ZC304022915, and research work for

partially funded by Zhejiang Normal University research fund YS304023947 and YS304023948.

Data collection and sharing for this project was funded by the Alzheimer's Disease Neuroimaging Initiative (ADNI) (National Institutes of Health Grant U01 AG024904) and DOD ADNI (Department of Defense award number W81XWH-12-2-0012). ADNI is funded by the National Institute on Aging, the National Institute of Biomedical Imaging and Bioengineering, and through generous contributions from the following: AbbVie, Alzheimer's Association; Alzheimer's Drug Discovery Foundation; Araclon Biotech; BioClinica, Inc.; Biogen; Bristol-Myers Squibb Company; CereSpir, Inc.; Cogstate; Eisai Inc.; Elan Pharmaceuticals, Inc.; Eli Lilly and Company; EuroImmun; F. Hoffmann-La Roche Ltd and its affiliated company Genentech, Inc.; Fujirebio; GE Healthcare; IXICO Ltd.; Janssen Alzheimer Immunotherapy Research & Development, LLC.; Johnson & Johnson Pharmaceutical Research & Development LLC.; Lumosity; Lundbeck; Merck & Co., Inc.; Meso Scale Diagnostics, LLC.; NeuroRx Research; Neurotrack Technologies; Novartis Pharmaceuticals Corporation; Pfizer Inc.; Piramal Imaging; Servier; Takeda Pharmaceutical Company; and Transition Therapeutics. The Canadian Institutes of Health Research is providing funds to support ADNI clinical sites in Canada. Private sector contributions are facilitated by the Foundation for the National Institutes of Health (www.fnih.org). The grantee organization is the Northern California Institute for Research and Education, and the study is coordinated by the Alzheimer's Therapeutic Research Institute at the University of Southern California. ADNI data are disseminated by the Laboratory for Neuro Imaging at the University of Southern California.

CREDIT AUTHORSHIP CONTRIBUTION STATEMENT

Atif Mehmood: Methodology, Writing – original draft. **Farah Shahid:** Methodology, Writing – review & editing. **Rizwan Khan:** Methodology, Formal analysis, Writing – review & editing. **Mostafa M. Ibrahim:** Writing – review & editing. **Zhonglong Zheng:** Funding acquisition, Conceptualization, Supervision, Writing – review & editing.

REFERENCES

Ahmed S, Choi KY, Lee JJ, Kim BC, Kwon GR, Lee KH, Jung HY (2019) Ensembles of patch-based classifiers for diagnosis of alzheimer diseases. IEEE Access 7:73373–73383. https://doi.org/10.1109/ACCESS.2019.2920011.

Amoroso N, Diacono D, Fanizzi A, La Rocca M, Monaco A, Lombardi A, Guaragnella C, Bellotti R, Tangaro S (2018) Deep learning reveals Alzheimer's disease onset in MCI subjects: results from an international challenge. J Neurosci Methods 302:3–9. https://doi.org/10.1016/j.jneumeth.2017.12.011.

Basaia S, Agosta F, Wagner L, Canu E, Magnani G, Santangelo R, Filippi M (2019) Automated classification of Alzheimer's disease and mild cognitive impairment using a single MRI and deep neural networks. NeuroImage: Clin 21. https://doi.org/10.1016/j.nicl.2018.101645 101645.

Billeci L, Badolato A, Bachi L, Tonacci A (2020) Machine learning for the classification of Alzheimer's disease and its prodromal stage using brain diffusion tensor imaging data: a systematic review. Processes 8(9). https://doi.org/10.3390/pr8091071.

Carcagnì P, Leo M, Del Coco M, Distante C, De Salve A (2023) Convolution neural networks and self-attention learners for Alzheimer dementia diagnosis from brain MRI. Sensors 23:(3). https://doi.org/10.3390/s23031694.

Chen Z, Wang Z, Zhao M, Zhao Q, Liang X, Li J, Song X (2022) A new classification network for diagnosing Alzheimer's disease in class-imbalance MRI datasets. Front Neurosci 16. https://doi.org/10.3389/fnins.2022.807085.

Deepa N, Chokkalingam SP (2022) Optimization of VGG16 utilizing the arithmetic optimization algorithm for early detection of Alzheimer's disease. Biomed Signal Process Control 74(2021). https://doi.org/10.1016/j.bspc.2021.103455 103455.

Ebrahimi A, Luo S, for the Alzheimer's Disease Neuroimaging Initiative (2021) Convolutional neural networks for Alzheimer's disease detection on MRI images. J Med Imaging 8(02):1–18. https://doi.org/10.1117/1.jmi.8.2.024503.

Faisal FUR, Kwon GR (2022) Automated detection of Alzheimer-s disease and mild cognitive impairment using whole brain MRI. IEEE Access 10:65055–65066. https://doi.org/10.1109/ACCESS.2022.3180073.

Ferreira LK, Rondina JM, Kubo R, Ono CR, Leite CC, Smid J, Bottino C, et al. (2018) Support vector machine-based classification of neuroimages in Alzheimer's disease: direct comparison of FDG-PET, RCBF-SPECT and MRI data acquired from the same individuals. Rev Bras Psiquiatr 40(2):181–191. https://doi.org/10.1590/1516-4446-2016-2083.

Franciotti R, Nardini D, Russo M, Onofrj M, Sensi SL (2023) Comparison of machine learning-based approaches to predict the conversion to Alzheimer's disease from mild cognitive impairment. Neuroscience 514:143–152. https://doi.org/10.1016/j.neuroscience.2023.01.029.

Friston KJ, Holmes AP, Worsley KJ, Poline J-P, Frith CD, Frackowiak RSJ (1994) Statistical parametric maps in functional imaging: a general linear approach. Hum Brain Mapp 2(4):189–210. https://doi.org/10.1002/hbm.460020402.

Gaser C, Dahnke R, Thompson PM, Kurth F, Luders E (2022) CAT – A computational anatomy toolbox for the analysis of structural MRI data. Biorxiv. 2022-06.

Grundman M, Sencakova D, Jack CR, Petersen RC, Kim HT, Schultz A, Weiner MF, et al. (2002) Brain MRI hippocampal volume and prediction of clinical status in a mild cognitive impairment trial. J Mol Neurosci 19(1–2):23–27. https://doi.org/10.1007/s12031-002-0006-6.

Gu J, Wang Z, Kuen J, Ma L, Shahroudy A, Shuai B, Liu T, et al. (2018) Recent advances in convolutional neural networks. Pattern Recogn 77:354–377. https://doi.org/10.1016/j.patcog.2017.10.013.

Hajamohideen F, Shaffi N, Mahmud M, Subramanian K, Sariri AA, Vimbi V, Abdesselam A (2023) Four-way classification of Alzheimer's disease using deep Siamese convolutional neural network with triplet-loss function. Brain Informatics 10(1). https://doi.org/10.1186/s40708-023-00184-w.

Hampstead BM, Stringer AY, Iordan AD, Ploutz-Snyder R, Sathian K (2022) Toward rational use of cognitive training in those with mild cognitive impairment. Alzheimer's and Dementia, 2021:933–945. https://doi.org/10.1002/alz.12718.

Hazarika RA, Kandar D, Maji AK (2023) A novel machine learning based technique for classification of early-stage alzheimer's disease using brain images. Multimed Tools Appl. https://doi.org/10.1007/s11042-023-16379-6.

Heising L, Angelopoulos S (2022) Operationalising fairness in medical ai adoption: detection of early Alzheimer's disease with 2D CNN. BMJ Health and Care Informatics 29(1):1–7. https://doi.org/10.1136/bmjhci-2021-100485.

Hu S, Yu W, Chen Z, Wang S (2020) Medical Image Reconstruction Using Generative Adversarial Network for Alzheimer Disease Assessment with Class-Imbalance Problem. In: 2020 IEEE 6th

International Conference on Computer and Communications, ICCC 2020, 1323–27. https://doi.org/10.1109/ICCC51575.2020.9344912

Ieracitano C, Mammone N, Bramanti A, Hussain A, Morabito FC (2019) A convolutional neural network approach for classification of dementia stages based on 2D-spectral representation of EEG recordings. Neurocomputing 323:96–107. https://doi.org/10.1016/j.neucom.2018.09.071.

Jack CR, Bernstein MA, Fox NC, Thompson P, Alexander G, Harvey D, Borowski B, et al. (2008) The Alzheimer's disease neuroimaging initiative (ADNI): MRI methods. J Magn Reson Imaging 27(4):685–691. https://doi.org/10.1002/jmri.21049.

Joy T, Rao MS, Madhyastha S (2018) N-acetyl cysteine supplement minimize tau expression and neuronal loss in animal model of Alzheimer's disease. Brain Sci 8(10):1–15. https://doi.org/10.3390/brainsci8100185.

Lin W, Tong T, Gao Q, Guo Di, Xiaofeng Du, Yang Y, Guo G, Xiao M, Min Du, Xiaobo Qu (2018) convolutional neural networks-based MRI image analysis for the Alzheimer's disease prediction from mild cognitive impairment. Front Neurosci 12(NOV):1–13. https://doi.org/10.3389/fnins.2018.00777.

Liu CF, Padhy S, Ramachandran S, Wang VX, Efimov A, Bernal A, Shi L, et al. (2019a) using deep siamese neural networks for detection of brain asymmetries associated with Alzheimer's disease and mild cognitive impairment. Magn Reson Imaging 64:190–199. https://doi.org/10.1016/j.mri.2019.07.003.

Liu M, Cheng D, Wang K, Wang Y (2018) Multi-modality cascaded convolutional neural networks for Alzheimer's disease diagnosis. Neuroinformatics 16(3–4):295–308. https://doi.org/10.1007/s12021-018-9370-4.

Liu M, Zhang J, Adeli E, DInggang Shen (2019b) Joint classification and regression via deep multi-task multi-channel learning for Alzheimer's disease diagnosis. IEEE Trans Biomed Eng 66 (5):1195–1206. https://doi.org/10.1109/TBME.2018.2869989.

Mehmood A, Abugabah A, AlZubi AA, Sanzogni L (2022) Early diagnosis of Alzheimer's disease based on convolutional neural networks. Comput Syst Sci Eng 43(1):305–315. https://doi.org/10.32604/csse.2022.018520.

Odusami M, Maskeliūnas R, Damaševičius R (2022) An intelligent system for early recognition of Alzheimer's disease using neuroimaging. Sensors 22:(3). https://doi.org/10.3390/s22030740.

Oktavian MW, Yudistira N, Ridok A (2023) Classification of Alzheimer's disease using the convolutional neural network (CNN) with transfer learning and weighted loss. IAENG Int J Comput Sci 50(3):1–10.

Pandey P, Khare A, Srivastava P (2022) Detection of Alzheimer's disease using CNN architectures. ADBU J Eng Technol 11 (1):1–6.

Park SW, Yeo NY, Kim Y, Byeon G, Jang JW (2023) Deep learning application for the classification of Alzheimer's disease using 18F-Flortaucipir (AV-1451) tau positron emission tomography. Sci Rep 13(1):1–11. https://doi.org/10.1038/s41598-023-35389-w.

Peng Z, Zhang HT, Wang G, Zhang J, Qian S, Zhao Y, Zhang R, Wang W (2022) Cerebral neurovascular alterations in stable chronic obstructive pulmonary disease: a preliminary FMRI study. PeerJ 10:1–18. https://doi.org/10.7717/peerj.14249.

Plachez C, Tsytsarev V, Zhao S, Erzurumlu RS (2023) Amyloid deposition and dendritic complexity of corticocortical projection cells in five familial Alzheimer's disease mouse. Neuroscience 512:85–98. https://doi.org/10.1016/j.neuroscience.2022.12.013.

Puig-Parnau I, Garcia-Brito S, Vila-Soles L, Riberas A, Aldavert-Vera L, Segura-Torres P, Kádár E, Huguet G (2023) Intracranial self-stimulation of the medial forebrain bundle ameliorates memory disturbances and pathological hallmarks in an Alzheimer's disease model by intracerebral administration of amyloid-β in rats. Neuroscience 512:16–31. https://doi.org/10.1016/j.neuroscience.2023.01.005.

Sethi M, Rani S, Singh A, Mazón JLV (2022) A CAD system for Alzheimer's disease classification using neuroimaging MRI 2D slices. Comput Math Methods Med 2022. https://doi.org/10.1155/2022/8680737.

Tinauer C, Heber S, Pirpamer L, Damulina A, Schmidt R, Stollberger R, Ropele S, Langkammer C (2022) Interpretable brain disease classification and relevance-guided deep learning. Sci Rep 12 (1):1–13. https://doi.org/10.1038/s41598-022-24541-7.

Vasant P, Ivan Z, Gerhard-Wilhelm W (2019) Intelligent Computing and Optimization: Proceedings of the 2nd International Conference on Intelligent Computing and Optimization 2019. Springer Nature. Available from: https://doi.org/10.1007/978-3-030-00979-3_56.

Wang H, Shen Y, Wang S, Xiao T, Deng L, Wang X, Zhao X (2019) Ensemble of 3D densely connected convolutional network for diagnosis of mild cognitive impairment and Alzheimer's disease. Neurocomputing 333:145–156. https://doi.org/10.1016/j.neucom.2018.12.018.

Wang JT, Gang Xu, Ren RJ, Wang Y, Tang R, Huang Q, Li JP, Al-Nusaif M, Le WD, Wang G (2022) The impacts of health insurance and resource on the burden of Alzheimer's disease and related dementias in the world population. Alzheimer's Dementia 2022:967–979. https://doi.org/10.1002/alz.12730.

Wang S, Wang X, Yong Hu, Shen Y, Yang Z, Gan M, Lei B (2021) Diabetic retinopathy diagnosis using multichannel generative adversarial network with semisupervision. IEEE Trans Autom Sci Eng 18(2):574–585. https://doi.org/10.1109/TASE.2020.2981637.

Wen J, Thibeau-Sutre E, Diaz-Melo M, Samper-González J, Routier A, Bottani S, Dormont D, Durrleman S, Burgos N, Colliot O (2020) Convolutional neural networks for classification of Alzheimer's disease: overview and reproducible evaluation. Med Image Anal 63. https://doi.org/10.1016/j.media.2020.101694.

Wu ZZ, Weise T, Wang Y, Wang Y (2020) Convolutional neural network based weakly supervised learning for aircraft detection from remote sensing image. IEEE Access 8:158097–158106. https://doi.org/10.1109/ACCESS.2020.3019956.

Xiao Y, Wang J, Huang K, Gao L, Yao S (2023) Progressive structural and covariance connectivity abnormalities in patients with Alzheimer's disease. Front Aging Neurosci 14 (January):1–11. https://doi.org/10.3389/fnagi.2022.1064667.

Xing X, Rafique MU, Liang G, Hunter Blanton Yu, Zhang CW, Jacobs N, Lin AL (2023) Efficient training on Alzheimer's disease diagnosis with learnable weighted pooling for 3D PET brain image classification. Electronics (Switzerland) 12(2):1–13. https://doi.org/10.3390/electronics12020467.

Yu W, Lei B, Wang S, Liu Y, Feng Z, Yong Hu, Shen Y, Michael KN (2023) Morphological feature visualization of Alzheimer's disease via multidirectional perception GAN. IEEE Trans Neural Networks Learn Syst 34(8):4401–4415. https://doi.org/10.1109/TNNLS.2021.3118369.

Zuo Q, Zhong N, Pan Yi, Huisi Wu, Lei B, Wang S (2023) Brain structure-function fusing representation learning using adversarial decomposed-VAE for analyzing MCI. IEEE Trans Neural Syst Rehabil Eng 31:4017–4028. https://doi.org/10.1109/TNSRE.2023.3323432.

(Received 18 October 2023, Accepted 10 March 2024)
(Available online 16 March 2024)